

***IMPACT OF ULTRASOUND ELASTOGRAPHY,  
IN THE DIAGNOSIS OF SOLID BREAST  
LESIONS.***

**Thesis**

**Submitted for partial fulfillment  
of the master degree in radiodiagnosis**

**By**

**Amany Abd Elhamid Abd Elhakam**

**Supervised by**

**Dr. Ahmed Mohamed Monib**

**Professor of Radiodiagnosis**

**Faculty of Medicine**

**Ain Shams University**

**Dr. Amr Mahmoud Abd ELsamad**

**Assistant professor of Radiodiagnosis**

**Faculty of Medicine**

**Ain Shams University**

**Faculty of Medicine**

**Ain Shams University**

**2018**

## ACKNOWLEDGEMENT

First and foremost, thanks to Allah, the most beneficial *and most merciful*.  
I am so grateful and most appreciative to the efforts of  
*Prof. Dr. Ahmed Mohamed Monib ,Professor of Radiodiagnosis, Faculty of Medicine,*  
*Ain Shams university .No* words can express what I owe to him for *his* endless  
patience, continuous advice and support.

*I am really indepted to Dr. Amr Mahmoud Abd ELsamad,*  
*Assistant professor in Radiodiagnosis, Ain Shams University,*  
*for his cooperation, and support, I would not have been able to complete*  
*this work, without his continuous help and great efforts.*

Finally,I am deeply thankful to my family *for their kind love which*  
allowed me to *complete this study* .

## ABSTRACT

*Breast cancer is a major health problem that warranted efforts to be paid in order to increase the diagnostic capability of the routinely used diagnostic aids. Ultrasound elastography is one of the newly introduced ultrasound built-in software that could increase the diagnostic capability of conventional ultrasound based on the fact that breast cancer is usually harder than benign breast lesions.*

*The routinely used method for classification of breast lesions according to tissue elasticity is the color coding as well as the strain ratio methods. Ultrasound elastography, does not only have a confirmatory diagnostic tool with sono-mammography, but also can be a beneficial technique by which ultrasound BIRADS downgrading of benign lesions could be elicited, thus reducing the number of unnecessary breast biopsies, and consequently improve the patients compliance .*

*However, ultrasound elastography has some limitations, such as operator dependency, inter, intraobserver variability, and results variability according to the internal structure of lesion being evaluated. So the cases should be evaluated as a whole regarding the history, clinical data, sono-mammographic findings, and ultrasound elastographic evaluation to attain the best diagnostic results, and to avoid false positive, and negative diagnoses.*

***Key words: Breast Lesions –Conventional Ultrasound – Ultrasound Elastography –Strain Ratio.***

## List of Abbreviations

<b>ACR</b>	<i>American Colleague of Radiology</i>
<b>ANDAI</b>	<i>Aberration of Normal Development And Involution</i>
<b>AUC</b>	<i>Area Under Curve</i>
<b>BGR</b>	<i>Blue Green Red</i>
<b>BIRADS</b>	<i>Breast Imaging Reporting And Data System</i>
<b>CC</b>	<i>Cranio- Caudal</i>
<b>C-plane</b>	<i>Coronal plane</i>
<b>CAM</b>	<i>Combined Auto-correlation Method</i>
<b>CD</b>	<i>Color Doppler</i>
<b>CEUS</b>	<i>Contrast Enhanced Ultrasound</i>
<b>CI</b>	<i>Confidence Interval</i>
<b>2-D</b>	<i>Two - Dimensional</i>
<b>3-D</b>	<i>Three - Dimensional</i>
<b>DCIS</b>	<i>Ductal Carcinoma In Situ</i>
<b>E</b>	<i>Elastoscore</i>
<b>FM</b>	<i>Fibrocystic Mastopathy</i>
<b>FN</b>	<i>False Negative</i>
<b>FNAC</b>	<i>Fine Needle Aspiration Cytology</i>
<b>IDC</b>	<i>Infiltrating Ductal Carcinoma</i>
<b>LIQ</b>	<i>Lower Inner Quadrant</i>
<b>L/T ratio</b>	<i>Longitudinal / Transverse axis ratio</i>
<b>LT.</b>	<i>Left</i>
<b>MLO</b>	<i>Medio Lateral Oblique</i>
<b>NPV</b>	<i>Negative Predictive Value</i>
<b>PPV</b>	<i>Positive Predictive Value</i>
<b>RT.</b>	<i>Right</i>
<b>ROC</b>	<i>Receiver Operating Characteristic Curve</i>
<b>ROI</b>	<i>Region Of Interest</i>
<b>SE</b>	<i>Sonoelastography</i>
<b>SR</b>	<i>Strain Ratio</i>
<b>SSI</b>	<i>Supersonic Shear Imaging</i>
<b>TA</b>	<i>Total Accuracy</i>
<b>TDLU</b>	<i>Terminal Ductal Lobular Unit</i>
<b>UE</b>	<i>Ultrasound Elastography</i>
<b>UOQ</b>	<i>Upper Outer Quadrant</i>
<b>US</b>	<i>Ultrasound</i>

## List of Figures

Figure number	Description	P
<b>Figure (1-1)</b>	Breast profile.	6
<b>Figure (1-2)</b>	Anatomy of the human breast, a lobe and a TDLU.	7
<b>Figure (1-3)</b>	Diagram of the lymphatic drainage of the upper limb and breast	9
<b>Figure (2-1)</b>	Fibroadenoma, cut surface of a pathological gross specimen.	11
<b>Figure (2-2)</b>	Cut surface of a macroscopic specimen of an invasive ductal carcinoma of the breast.	14
<b>Figure (2-3)</b>	Gross specimen of intracystic papillary carcinoma.	16
<b>Figure (3-1)</b>	Normal sonographic (three zonal) anatomy of the breast.	20
<b>Figure (3-2)</b>	Adjacent breast carcinoma and fibroadenoma.	22
<b>Figure (3-3)</b>	Fibroadenomas (sonogram).	24
<b>Figure (3-4)</b>	Breast fibroadenoma with macrocalcifications(sonogram).	25
<b>Figure (3-5)</b>	Young” fibroadenoma(sonogram).	25
<b>Figure (3-6)</b>	Phylloides tumor (sonogram).	26
<b>Figure (3-7)</b>	Breast abscess (sonogram).	27
<b>Figure (3-8)</b>	Intracystic carcinoma of the breast(sonogram)	27
<b>Figure (3-9)</b>	Morpho-structural pattern of breast cysts.	28
<b>Figure (3-10)</b>	lipomas of the breast (sonogram).	29
<b>Figure (3-11)</b>	breast hemangioma (sonogram)	29
<b>Figure (3-12)</b>	Fat necrosis of the breast (sonogram)	03
<b>Figure (3-13)</b>	Radial scar (sonogram)	31
<b>Figure (3-14)</b>	Breast Sonogram and and power Doppler of ductal carcinoma in situ.	31
<b>Figure (3-15)</b>	Breast invasive ductal carcinoma (sonogram).	32
<b>Figure (3-16)</b>	Medullary carcinoma of the breast (sonogram).	33
<b>Figure (3-17)</b>	Breast mucinous carcinoma (sonogram).	34
<b>Figure (3-18)</b>	Inflammatory carcinoma of the breast (sonogram).	35
<b>Figure (3-19)</b>	Carcinomatous mastitis (sonogram).	36
<b>Figure (3-20)</b>	Main color doppler patterns of focal breast lesions.	
<b>Figure (4-1)</b>	The principle of Elastography.	36
<b>Figure (4-2)</b>	Generation of a conical shear wave front propagating in the imaging plane of the echographic probe.	39
<b>Figure (4-3)</b>	Ultrasound elastography of invasive ductal carcinoma. (lesion size comparison method)	40
<b>Figure (4-4)</b>	ultrasound elastography of benign stromal fibrosis(lesion size comparison method)	
<b>Figure (4-5)</b>	Tsukuba scoring system illustration.	41
<b>Figure (4-6)</b>	Sonoelastographic classification by the Italian Multi-Center Team (modification of the Tsukuba score).	43
<b>Figure (4-7)</b>	Breast mass classification using scores and the assessment of color variation during compression and after decompression of the breast tissue.	44
<b>Figure (4-8)</b>	Strain ratio (SR) assessment.	45
<b>Figure (4-9)</b>	Ultrasound elastographic image of an invasive ductal carcinoma by both color coding and strain ratio methods.	46
<b>Figure (4-10)</b>	Inappropriate and appropriate degrees of breast compression	47
<b>Figure (4-11)</b>	Elastographic images obtaining during appropriate ,and inappropriate degree of compression.	48
<b>Figure (4-12)</b>	Sonogram and elastogram of a normal breast.	49
		50

<b>Figure (5-1)</b>	Elastogram and strain ratio of a fibroadenoma.	52
<b>Figure (5-2)</b>	Fibroadenoma elastogram with elasticity score of 2.	52
<b>Figure (5-3)</b>	Real time ultrasound elastography of a hyalinized fibroadenoma, with exuberant stromal collagen content.	53
<b>Figure (5-4)</b>	Elastographic image of a mastopathic nodule.	54
<b>Figure (5-5)</b>	Sonogram and elastogram of Scirrhus type invasive ductal carcinoma.	55
<b>Figure (5-6)</b>	Elastogram and strain ratio display of an invasive ductal carcinoma .	55
<b>Figure (5-7)</b>	Sono-elastograms of ductal infiltrating carcinoma with atypical US features.	56
<b>Figure (5-8)</b>	Sono-elastogram of Lobular invasive carcinoma.	56
<b>Figure (5-9)</b>	Elastogram and strain ratio display of Lobular invasive carcinoma.	57
<b>Figure (5-10)</b>	Sono-elastogram of a complicated cyst.	58
<b>Figure (5-11)</b>	Sono-elastogram of intra-cystic papilloma	59
<b>Figure (5-12)</b>	Comparison between B-mode image and quantitative elasticity map of a simple cyst.	60
<b>Figure (5-13)</b>	Elastographic images of benign and malignant lymph nodes.	61
<b>Figure (5-14)</b>	Magnified mediolateral oblique mammogram ,and sonoelastogram images of breast microcalcifications(benign).	62
<b>Figure (5-15)</b>	Magnified cranio-caudal mammogram demonstrates and sonoelastogram images of breast microcalcifications (malignant).	66
<b>Figure (5-16)</b>	Sono-elastogram of an Epidermal cyst.	64
<b>Figure (5-17)</b>	Fibroadenoma (BI-RADS 4) and elasticity score 2.	64
<b>Figure (5-18)</b>	Fibroadenoma (BI-RADS 3) and elasticity score 1.	65
<b>Figure (5-19)</b>	Breast lesion (BIRADS 2), and elasticity images of chromatic tri-stratification pattern.	66
<b>Figure (5-20)</b>	Real time ultrasound elastography of a Fat necrosis (Tsukuba elasticity score 5)	67
<b>Figure (5-21)</b>	Calcified fibroadenoma(Tsukuba elasticity score 4).	67
<b>Figure (6-1)</b>	Power Doppler images of a breast lesion before and after ultrasound contrast media injection.	69
<b>Figure (6-2)</b>	Ultrasound and MicroPure images of microcalcifications in invasive ductal carcinoma.	72
<b>Figure (6-3)</b>	Ultrasound and MicroPure images of diffuse benign microcalcifications.	72
<b>Figure (6-4)</b>	Two and Three dimensional sonograms of a ductal filling defect, showing the solid extent of the ductal involvement.	74
<b>Figure (8-1)</b>	Graph illustrates the Final pathologic diagnoses of breast lesions.	82
<b>Figure (8-2)</b>	graph illustrates the number and percentage of breast lesions for each US BIRADS category	84
<b>Figure (8-3)</b>	Graph illustrates the distribution of different elastography scores	88
<b>Figure (8-4)</b>	Graph illustrates sensitivity,specificity,TA, PPV,and NPV for elastography at different cut off points.	89
<b>Figure (8-5)</b>	Receiver-operating characteristic curves for the strain ratio measurement method	91
<b>Figure (8-6)</b>	graph illustrates sensitivity ,specificity, TA, PPV, NPV(when SR<3.13 (benign), SR ≥3.13 (malignant )).	92
<b>Figure (8-7)</b>	Graph illustrates Sensitivity, specificity, PPV, NPV of elastography and SR, for lesions < 20 mm and ≥20mm.	95
<b>Figure (8-8)</b>	Graph illustrates areas under ROC curves, for conventional ultrasound, elastoscoring and strain ratio methods.	96

<b>Figure (9-1)</b>	Case 1: (A) B-mode ultrasound	100
	(B) Elastographic image of fibroadenoma.	101
<b>Figure (9-2)</b>	Case 2: (A) B-mode ultrasound	102
	(B) Elastographic image of partially calcified fibroadenoma.	103
<b>Figure (9-3)</b>	Case 3: (A) B-mode ultrasound, and	104
	(B) Elastography image of highly cellular fibroadenoma.	104
<b>Figure (9-4)</b>	Case 4: (A) Bilateral medio-lateral oblique mammograms	105
	(B) Bilateral craniocaudal mammograms, (C) selected tomosynthesis cuts	106
	(D) B-mode ultrasound (E) color Doppler image	107
	(F) Elastographic image of Multifocal infiltrating ductal carcinoma.	108
	(G) B-mode ultrasound of axillary lymphadenopathy	108
<b>Figure (9-5)</b>	Case 5: (A) B-mode ultrasound and	109
	(B) Elastographic image of grade III infiltrating ductal carcinoma.	110
<b>Figure (9-6)</b>	Case 6: (A) Bilateral craniocaudal mammograms,	111
	(B) Bilateral medio-lateral oblique mammograms, (C) B-mode ultrasound,	112
	(D) Color Doppler, (E) B-mode ultrasound of axillary lymphadenopathy, and	113
	(F) Elastographic image of ductal carcinoma in situ.	114
<b>Figure (9-7)</b>	Case 7: (A) B-mode ultrasound,	115
	(B) Color Doppler, (C) B-mode ultrasound of axillary lymphadenopathy, and	116
	(D) Elastographic image of non-specific granulomatous mastitis.	117
<b>Figure (9-8)</b>	Case 8: (A) B-mode ultrasound, and	118
	(B) Elastographic image of focal breast adenosis.	119
<b>Figure (9-9)</b>	Case 9: (A) B-mode ultrasound, and	120
	(B) Elastographic image of lactating adenoma.	121
<b>Figure (9-10)</b>	Case 10: (A) Left breast mammogram (cranio-caudal, and mediolateral oblique views )	122
	(B) B-mode ultrasound, and (C) Elastographic image of infiltrating ductal carcinoma	123
<b>Figure (9-11)</b>	Case 11: (A) Right breast mammogram (cranio-caudal, and mediolateral oblique views ),	124
	(B) B-mode ultrasound, and (C) Elastographic image of infiltrating ductal carcinoma (non-schirrous variant).	125

# Table of Contents

<b>Contents.....</b>	
<b>➔Review of Literature.....</b>	
<i>Introduction and Aim of Work.....</i>	
<i>Anatomy of the Breast.....</i>	
<i>Pathological Entities of Different Breast Lesions.....</i>	
<i>Conventional Breast Ultrasound.....</i>	
<i>Ultrasound Elastography of the Breast .....</i>	
<i>Elastographic Features of Different Pathological Breast Entities....</i>	
<b>➔ Patients and Methods .....</b>	
<b>➔ Results .....</b>	
<b>➔ Case Presentation.....</b>	
<b>➔ Discussion.....</b>	
<b>➔ Summary and Conclusion.....</b>	
<b>➔ References.....</b>	
<b>➔ Arabic Summary .....</b>	



## Introduction and Aim of Work

Breast cancer is the most common female neoplasm (31% of tumors in females), and the second-leading cause of death among women. Breast lesions were first classified as malignant or benign categories (*Catalano et al, 2009*).

The most prevalent malignant lesions were further subdivided into three subgroups including: ductal carcinoma in situ (DCIS), invasive ductal carcinoma of nonscirrhous type, and invasive ductal carcinoma of scirrhous type (*Itoh et al, 2006*). Similarly, the most prevalent benign lesions were divided into three subgroups, including intraductal papilloma, fibroadenoma, and aberrations of normal development and involution (ANDI) (*Itoh et al, 2006*).

There have been marked advances in the quality of ultrasound imaging over the past 2 decades (*Zhi et al, 2007*). However the breast nodule is still a daily challenge for the radiologist in the setting of US diagnosis. This created the need for new diagnostic approaches including ultrasound elastography (UE) (*Catalano et al, 2009*).

The principle of elastography is that tissue compression produces strain (displacement) within the tissue, and that the strain is smaller in harder tissue than in softer tissue (*Itoh et al, 2006*). Therefore, by measuring the tissue strain induced by compression, ultrasound elastography (UE) can make the hardness of the tissue “visualize”, display its texture, and reflect the biological

characteristics of the mass. It shows promising prospects in differentiating benign from malignant breast tumor (*Zhang et al, 2009*).

Today, real time elastographic systems that allow freehand scanning and provide excellent spatial resolution with less noise are integrated into commercially available US units. Benign tumors show even strain, whereas breast cancers show no strain in lesions or in surrounding areas (*Cho et al, 2008*). Elastography could also be used to distinguish an area of shadowing due to fibrosis from that due to carcinoma (*Tan et al, 2008*).

The elastography strain images were scored according to the elasticity score in to five categories (*Tan et al, 2008*). Elasticity of breast tissue is affected by both physiological and pathological processes that cause structural changes as well as histological type of the mass being examined. Other factors that may affect the elasticity score are lesion size and depth. The more superficial the lesion, and the smaller its size, the more the sensitivity and specificity of yielded elastograms (*Regini et al, 2010*).

Elastography allows for differentiation of malignant lesions from benign lesions (even among lesions smaller than 10 mm) (*Itoh et al, 2006*). Also it has the potential to evaluate the nature of the lesions detected at screening mammography and associated with microcalcifications, whether benign or malignant (*Cho et al, 2009*).

Axillary lymphadenopathies are the single most important prognostic factor for operable breast cancer (*Catalano et al, 2009*). Elastography can provide useful information about the nature of lymph nodes and the quantitative

technique of the elastography further makes the diagnosis more accurate than B-mode, color and power Doppler sonography alone (*Zhang et al, 2009*).

Frequently cystic alterations of the breast are interpreted as indeterminate nodules by the conventional approach, particularly those with a thick fluid content, fine debris in suspension, or complex cysts with mural nodules (*Fleury et al, 2008*).

Combination between UE, conventional sonography, and mammography facilitate detection of two features of a lesion, morphologic characteristics and hardness, which reflect the properties of the lesion, facilitating differentiation between benign and malignant tumors, and thus elevating the sensitivity, specificity, accuracy, and the positive predictive value, augmenting the diagnostic capability of sonomammography (*Zhi et al, 2007*).

UE is better than sonomammography for detecting breast cancer in small sized breasts (*Zhi et al, 2007*). Also elastography has a higher sensitivity compared with B-mode US in the presence of breast lipomatous involution (*Thomas et al, 2006*). However, when using UE, one should pay attention to all the factors that would affect the stiffness of lesions such as large-scale necrosis, coarse calcifications, or organized hemorrhage, which may increase the hardness of the lesion, and cause misleading results (*Zhi et al, 2007*).

Elastography was found to be superior to B-mode US in evaluating BI-RADS 3 (**Breast Imaging Reporting and Data System**) benign lesions (*Thomas et al, 2006*). Prevention of unnecessary histopathologic confirmation of breast lesions of BI-RADS 3 or 4 corresponding with elasticity scores 2, is one of the most important advantages. Additionally, a 6-month follow-up is

not necessary in case of BI-RADS 3 in conventional B-mode US and elasticity scores 2. Both situations provide a downgrading of the lesion to category BI-RADS 2. This may support the compliance of women, and also reduces costs in the health care system (*Schaefer et al, 2011*).

There is very good inter-observer agreement in evaluating elastograms, which makes the method amenable to standardized interpretation (*Thomas et al, 2006*), however some authors documented that the inter-observer variability and image quality can influence performance. Future research will be critical to understand whether training and experience can ameliorate these effects (*Burnside et al, 2007*).

Sonoelastography is not, however, free of limitations. These include high level of operator dependency, subjective interpretation of elastograms and sensitivity to slight changes in patient position (*Regini et al, 2010*). In summary, recent improvements in breast ultrasound equipment technology have occurred including the introduction of UE, which is very promising complementary diagnostic tool. Breast ultrasound is still being developed further, and this will lead to further better diagnostic approaches (*Tohno et al, 2008*).

### **Aim of work**

The aim of this study is to detect the impact of ultrasound elastography in diagnosis of solid breast lesions, and to evaluate its capability in differentiating benign from malignant lesions, with special focus on:

A-Evaluation of sensitivity and specificity of sonoelastography, with cyto-histological diagnosis taken as the reference.

B-Detection of the ability of sonoelastography to provide additional information on tissue elasticity in the event of equivocal mammographic and/or sonographic findings in order to guide the diagnostic workup towards biopsy or follow-up.

## Anatomy of the Breast

The breast or mammary gland is a modified sweat gland that has the specific function of milk production (*De Paredes, 2007*).

The adult breast is composed of three basic structures: the skin, the subcutaneous fat, and the breast tissue, which includes the parenchyma and the stroma. Beneath the breast is the pectoralis major muscle, the breast parenchyma is enveloped by deep and superficial fascial layers; Cooper's ligaments, the fibrous strands that support the breasts, traverse the parenchyma and attach to the fascial layers. The parenchyma is divided into 15 to 20 segments, with each drained by a lactiferous duct (**Fig. 1-1**). The lactiferous ducts converge beneath the nipple, with about 5 to 10 major ducts draining into the nipple. Each duct drains a lobe composed of 20 to 40 lobules (*De Paredes, 2007*).

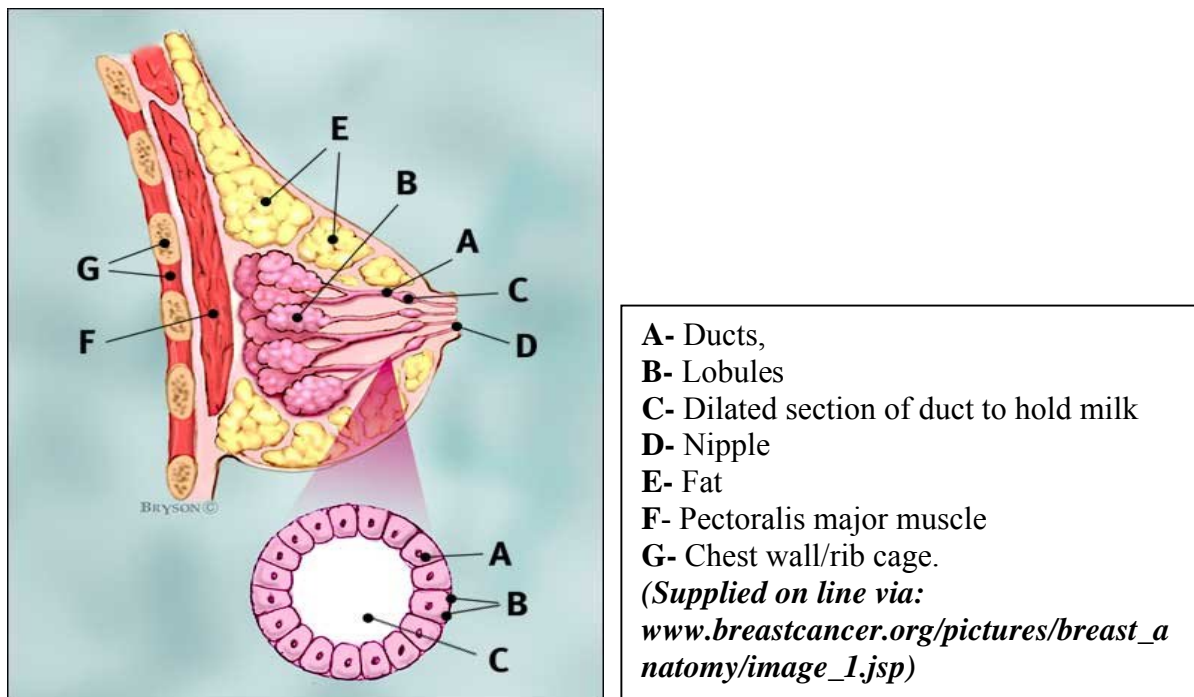


**Figure (1-1)** Breast profile:

**Wellings & Wolfe** further classified the microstructure of the normal breast into the terminal duct lobular unit (TDLU) (**Fig. 1-2**). Small branches of the lactiferous ducts lead into terminal ducts that drain a single lobule. The terminal duct is composed of the extralobular segment and the intralobular segment. The lobule is composed of the intralobular terminal duct and the blindly ending ductules (**Wellings & Wolfe 1978**). The ductules are lined by a single layer of epithelial cells and a flattened peripheral layer of myoepithelial cells. A loose fibrous connective tissue stroma supports the ductules of the lobule (**Wellings & Wolfe, 1978**).

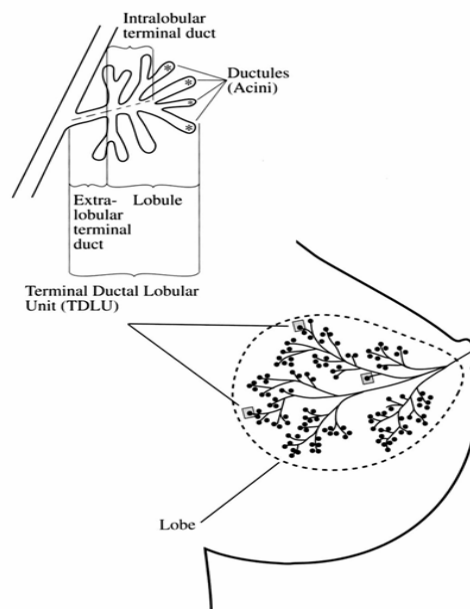


**Figure (1-2):** Anatomy of the human breast, a lobe and a TDLU.

(Supplied on line via: [herkules.oulu.fi/isbn9514270525/html/c161.html](http://herkules.oulu.fi/isbn9514270525/html/c161.html))

### Blood Supply and Lymphatic Drainage

The *primary arterial supply* to the breast is from the perforating branches of the internal mammary and lateral thoracic arteries. Minor contributions to the blood come from the branches of the thoracoacromial, subscapular, and thoracodorsal arteries. *Venous drainage* is primarily via branches of the internal mammary, intercostal, and axillary veins. The venous drainage of the breast is mainly to